

Rock physics properties from seismic attributes with global optimization methods

Qi Hu and Kris Innanen

ABSTRACT

The estimation of rock physics properties from seismic attributes is a nonlinear inverse problem. We investigate three global optimization methods: simulated annealing, genetic algorithm, and neighborhood algorithm for solving this problem. The input data are P-wave velocity, S-wave velocity, and density, and the rock physics properties to estimate are porosity, clay content, and water saturation. The two parameter sets are connected by an assumed rock physics model. Numerical examples are suggestive that the neighborhood algorithm is most efficient for improving data fit for the experiment we set up; porosity and clay content can be accurately estimated, whereas the water saturation estimate is prone to large errors. We explain this as a consequence of the low sensitivity of velocities and density to this property. However, simultaneous inversion for the whole set of the rock physics properties is problematic if the input data are erroneous. Consequently, we restrict the inversion to porosity and clay content only and assume a priori information of the exact water saturation. This makes the inversion stable with noisy data. Finally, we illustrate the application of the proposed global optimization method using the high-resolution results of elastic full waveform inversion (EFWI).

INTRODUCTION

In seismic reservoir characterization, the estimation of rock and fluid properties is generally achieved in two steps: seismic inversion and rock physics inversion (Bosch et al., 2010; Grana, 2016). In seismic inversion, we invert the seismic data (e.g., amplitude, time, waveforms) for the elastic model, such as velocities, density and elastic moduli. Seismic inversion can be performed using complex forward models and inverse algorithms, for example, full-waveform inversions (Tarantola, 2005; Brossier et al., 2009; Pan et al., 2018), or using methods that are less computationally intense such as AVO (amplitude versus offsets) inversions (Buland and Omre, 2003). In rock physics inversion, we invert the elastic attributes obtained from seismic inversion to estimate a model of rock properties, such as porosity, lithology, and fluid saturations (Doyen, 2007; Mavko et al., 2009). The relations between elastic attributes and rock properties are generally nonlinear, therefore, the inversion requires nonlinear optimization algorithms, such as gradient-based (local optimization) methods (Nocedal and Wright, 2006), or global optimization algorithms, such as simulated annealing and genetic algorithms (Sen and Stoffa, 2013).

For the rock physics inversion, the misfit surface as a function of rock physics parameters that are described by the mismatch between the predicted and observed elastic attributes may be complicated and characterized by multiple hills and valleys. Local optimization algorithms such as gradient-based methods typically attempt to find a local minimum in the close neighborhood of the starting model. Thus these algorithms will miss the global minimum if the starting solution is nearer to one of the local minima than the global minimum (Sen and Stoffa, 2013). By contrast, the global optimization methods such as

simulate annealing and genetic algorithm involve the random sampling of the whole model space, avoiding the convergence toward a local minimum (Dupuy et al., 2016).

The main factor that has slowed the application of global optimization algorithms to geophysical problems is their high computational demand. For example, If each model parameter can take M possible discrete values and there are N model parameters, then there are M^N possible models to be tested. Typically, model spaces of the order of 50^{50} or higher are common (Sen and Stoffa, 2013). Therefore, it is impractical to apply these methods to geophysical problems such as elastic full waveform inversion (EFWI), given the high cost of forward modeling and the large dimensionality of the model. However, for the rock physics inversion, the computational burden can be significantly alleviated. One reason is that the solutions of rock physics modeling are generally analytical, so the forward process is very fast. Another reason is that the elastic attributes of a specific grid point of model space is uniquely decided by the rock physics parameters of this point, therefore the transformation from elastic to rock properties can be done point by point. This allows a parallel computation for multiple grid points of small model dimensionality.

We investigate several well-developed global optimization methods for the rock physics inversion problem. Our goal is to seek an optimal solution which is corresponding to the lowest data misfit, although these methods can be applied as well in a statistical framework to estimate the uncertainties in the derived result. The report is structured as follows: first, we describe the underlying fundamental principles on which these algorithms are based; second, we conduct a single-point test for each algorithm. The velocities and density of a sample computed by rock physics modeling is used as input to estimate its rock physics properties. Then, we test the selected algorithm on pseudo-well logs to examine how errors in the input data affect the inversion. Finally, we combine EFWI for elastic attributes and the global optimization scheme to predict rock physics properties.

THEORIES AND METHODS

The inverse problem consists in the extraction of models (rock physics parameters) from input data (elastic attributes) and is formulated as

$$\mathbf{d} = g(\mathbf{m}). \quad (1)$$

In our approach, the model vector \mathbf{m} comprises of three rock physics parameters: porosity, clay content, and water saturation (P, C, Sw); the data vector comprises of three elastic parameters: P-wave velocity, S-wave velocity and density (V_P, V_S, ρ); the function g is a rock-physics relation: the KT model (Kuster and Toksöz, 1974). This function is nonlinear and the inverse of g cannot be computed. The solution of the system has to be obtained by optimization methods. In our case, computation of the forward model is very fast (computation of analytical relations) and the number of model parameters is low (three for a point-by-point inversion).

The optimization aims to minimize a scalar function (misfit function) describing the discrepancy between the observed data \mathbf{d}_{obs} and calculated data $g(\mathbf{m})$ (by forward model-

ing). We use the L_2 norm to compute the misfit as

$$E(\mathbf{m}) = \frac{1}{2}[(\mathbf{d}_{\text{obs}} - g(\mathbf{m}))^T C_d^{-1}(\mathbf{d}_{\text{obs}} - g(\mathbf{m}))], \quad (2)$$

where C_d^{-1} is the data covariance matrix, which contains information on data uncertainties.

We study three global optimization methods: simulated annealing (SA), genetic algorithm (GA) and neighborhood algorithm (NA). They belong to the category of directed Monte Carlo methods. Unlike the uniform Monte Carlo method, which by definition is a completely blind search since each new sample is independent of the previous samples, the three algorithms make use of previous samples to guide their search. We also note that each algorithm has several variants developed to speed up its convergence, for example, heat bath SA, fast SA, and GA with multipoint crossover, we use in this work their most basic versions.

Simulated Annealing

SA is based on an analogy with the physical process of annealing, which occurs when a solid in a heat bath is initially heated by increasing the temperature such that all the particles are distributed randomly in a liquid phase. This is followed by slow cooling such that all the particles arrange themselves in the low-energy ground state where crystallization occurs. In geophysical inverse problems, the energy function is identified with the objective function $E(\mathbf{m})$ (equation 2). We are interested in finding the state (or model) to minimize this function.

SA is implemented using an algorithm that simulates the physical annealing process. SA based on the Metropolis algorithm can be described as follows (adopted from course materials of Dr. Jan Dettmer):

- 1) Pick starting model \mathbf{m} with upper and lower bounds for all parameters, and starting temperature T .
- 2) Perturb \mathbf{m} to \mathbf{m}' , therefore, the difference in the energy between the two states $\Delta E = E(\mathbf{m}') - E(\mathbf{m})$.
- 3) Accept or reject \mathbf{m}' as a new state according to:
 - a. if $\Delta E \leq 0$, accept, $\mathbf{m} = \mathbf{m}'$.
 - b. if $\Delta E > 0$, draw random number $\xi \sim U(0, 1)$.
 - i. If $\xi \leq \exp(-\Delta E/T)$, accept, $\mathbf{m} = \mathbf{m}'$.
 - ii. if $\xi > \exp(-\Delta E/T)$, reject \mathbf{m}' and return to \mathbf{m} .
- 4) Repeat steps 1 and 2 many times and periodically reduce T by a small amount.

Therefore, SA provides a random walk that always accepts a downhill step (in E) and sometimes accepts an uphill step (allows escape from local minima). As T reduces, probability of accepting uphill steps decreases, and our search spends more time in regions of

minima, but can climb out. As T approaches zero, probability of accepting uphill steps also approaches zero, and eventually no more downhill steps are available, leading SA converge.

Genetic Algorithm

GA is based on an analogy with the processes of biologic evolution. Unlike SA, an initial population of models is selected at random, and the GA seeks to improve the fitness of the population generation after generation. This is principally accomplished by the genetic processes of selection, crossover, and mutation (Sen and Stoffa, 2013). Also, because GA works with models that are coded in some suitable form, we need to design a coding scheme that represents the model parameters. The basic steps of GA are:

- 1) Coding. In the simple binary coding scheme, each bit corresponds to a gene that can take a value of 0 or 1, and each individual in the population is completely described by its bit string or chromosome.
- 2) Selection. Once the fitness (data fit) of each individual model in the population is determined, the selection pairs individual models for reproduction. Models with higher fitness values are more likely to get selected.
- 3) Crossover. Once the models are selected and paired, crossover allows genetic information between the paired models to be shared. New models will be generated via the exchange of some information between the paired models.
- 4) Mutation. Mutation is the random alteration of a bit, which represents a random walk in model space.

After mutation, a new population of models is generated, and it often contain new models and some which are identical to previous models. We then repeat the genetic processes, i.e., from step 2) to step 4), many times to update the population.

Neighborhood Algorithm

NA is proposed by Sambridge (1999), which was motivated by a fundamental question: How can a search for new models be best guided by all previous models for which the forward problem has been solved (and hence the data misfit evaluated). To address this, NA makes use of the geometrical constructs known as Voronoi cells to derive the search in model space. Each cell is simply the nearest neighbor region about one of the previous samples. For example, the Voronoi cell about point \mathbf{m}_i is given by

$$V(\mathbf{m}_i) = \{\mathbf{x} \mid \|\mathbf{x} - \mathbf{m}_i\|_2 \leq \|\mathbf{x} - \mathbf{m}_j\|_2 \text{ for } j \neq i\}. \quad (3)$$

The algorithm uses the spatial properties of Voronoi cells to directly guide the sampling of parameter space. It can be summarized in four steps:

- 1) Generate an initial set of n_s models uniformly (or otherwise) in parameter space;

- 2) Calculate the misfit function for the most recently generated set of n_s models and determine the n_r models with the lowest misfit of all models generated so far;
- 3) Generate n_s new models by performing a uniform random walk in the Voronoi cell of each of the n_r chosen models (i.e. n_s/n_r samples in each cell);
- 4) Go to step 2.

The philosophy behind the algorithm is that the misfit of each of the previous models is representative of the region of space in its neighborhood (defined by its Voronoi cell). Therefore at each iteration new samples are concentrated in the neighborhoods surrounding the better data-fitting models. In this way the algorithm exploits the information contained in the previous models to adapt the sampling.

NUMERICAL EXAMPLES

Single-point test

We consider a sample with porosity, clay content and water saturation of 0.1, 0.2, and 0.3, respectively. The corresponding elastic response, P-wave velocity, S-wave velocity, and density, are computed by rock physics modeling based on the KT model, namely $(V_P, V_S, \rho) = \text{KT}(P, C, S_w)$. The ranges of possible values in model space are $0 \leq P \leq 0.4$, $0 \leq C \leq 1$, and $0 \leq S_w \leq 1$. The example is chosen to illustrate how the three algorithms work to predict the model $\mathbf{m} = (P, C, S_w)$ from the data $\mathbf{d} = (V_P, V_S, \rho)$. Notably, no exhaustive testing was done and we do not expect the values to be in any way perfect. If an extremely large number of random walks is allowed, each algorithm can resemble a grid-search method, which involves searching through every point in model space, but this is not usually a practical approach.

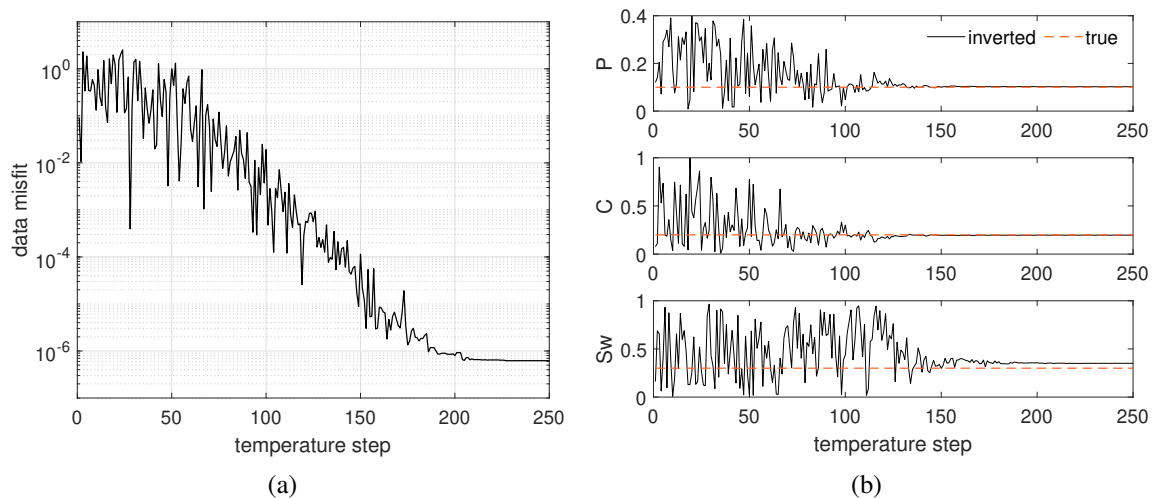


FIG. 1. Simulation results using Metropolis SA. Variations of (a) data misfit and (b) the inverted model as a function of temperature.

Figure 1 shows the evolution of data misfit and the inverted model using Metropolis SA. We employ a cooling schedule $T_k = T_0(0.9)^k$, where T_0 is the starting temperature and k

is the temperature step (or iteration number). The starting temperature $T_0 = 200$ is picked so that most random walks are accepted in the beginning of simulation. As the temperature reduces, the probability of accepting uphill steps decreases (Figure 1a). Eventually the algorithm converges to near the global optimal solution within 250 iterations. The porosity and clay content are correctly estimated, whereas the inverted water saturation deviates slightly from its true value.

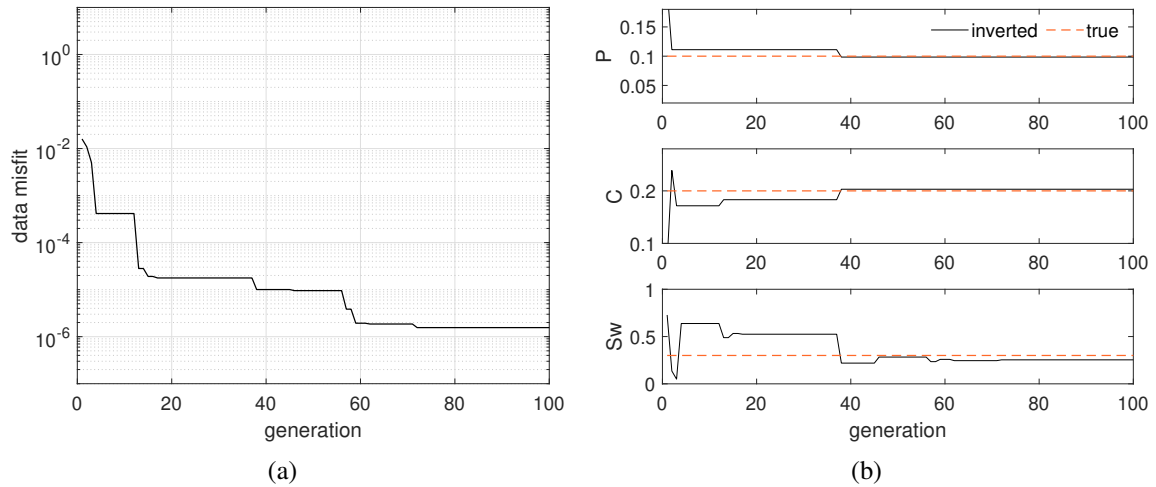


FIG. 2. Simulation results using GA. Evolution of (a) data misfit and (b) the best-fit model.

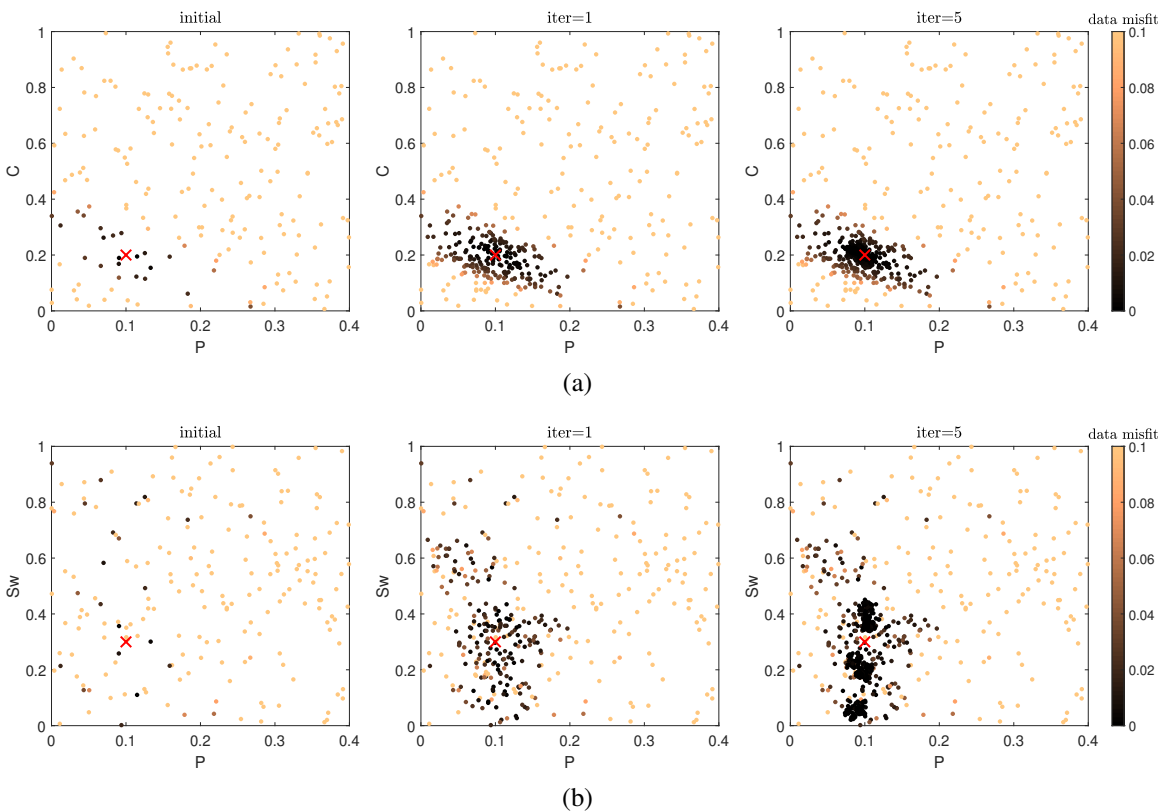


FIG. 3. Simulation results using NA. The dots represent the models produced by NA and are color-coded by data misfit. The true model is denoted by the red cross.

Figure 2 shows the simulation process using GA. We use a population size of 100 models, a crossover probability of 0.5, and a mutation probability of 0.5. Unlike the SA curve (Figure 1a) where an uphill step is allowed, in GA the best-fit model of the current generation is saved for the next generation, making GA always converge toward models with lower data misfit (Figure 2a). The best-fit model is reasonably good after 100 iterations.

Figure 3 illustrates the process of searching the model space using NA. At each iteration the NA generates 200 samples of a uniform random walk inside each of the Voronoi cells of the current five best models (i.e. $ns = 200$, $nr = 5$). The initial 200 samples are generated randomly. As the algorithm proceeds, the information in the misfit-surface is exploited to concentrate sampling in the regions where the misfit is low. Consequently, the porosity and clay content are well estimated, with only one main minimum located close to the true value in the $P - C$ space. However, the water saturation is not well estimated, displaying several local minimum.

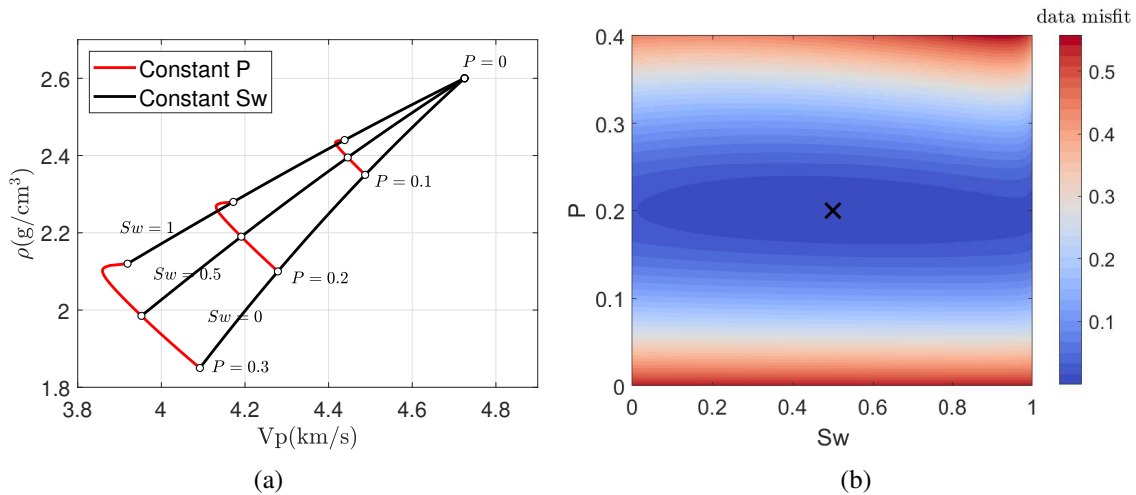
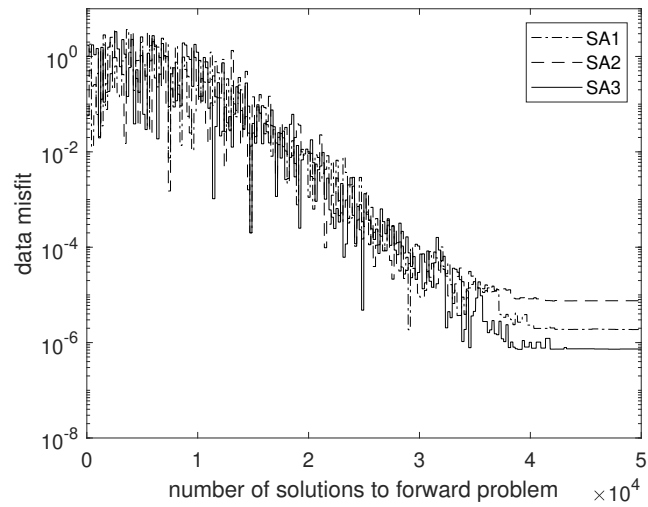


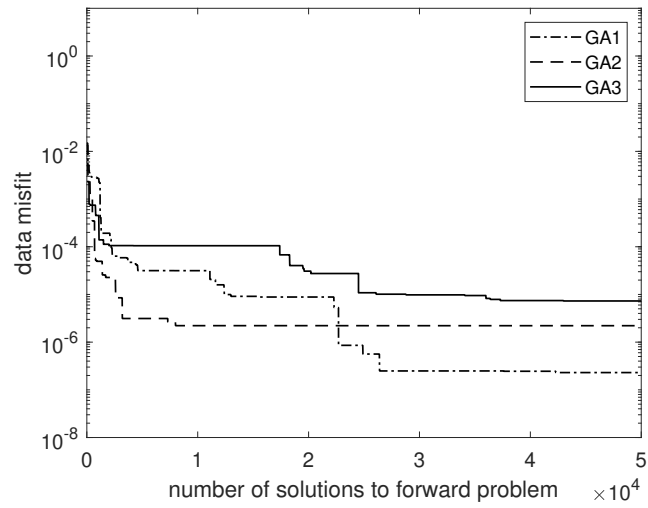
FIG. 4. Sensitivity study. Variations of (a) velocity and density and (b) data misfit as a function of porosity and water saturation.

We observe in the preceding example that water saturation is more difficult to estimate than porosity and clay content. This is explained in Figure 4. The rock physics template in Figure 4a is generated by fixing C and calculating the velocity and density for each combination of P and Sw . It illustrates that V_P and ρ are far more sensitive to P than to Sw (note that the Sw is given a wider range). The contour plot in Figure 4b reveals that the misfit function has a flat trough with respect to Sw .

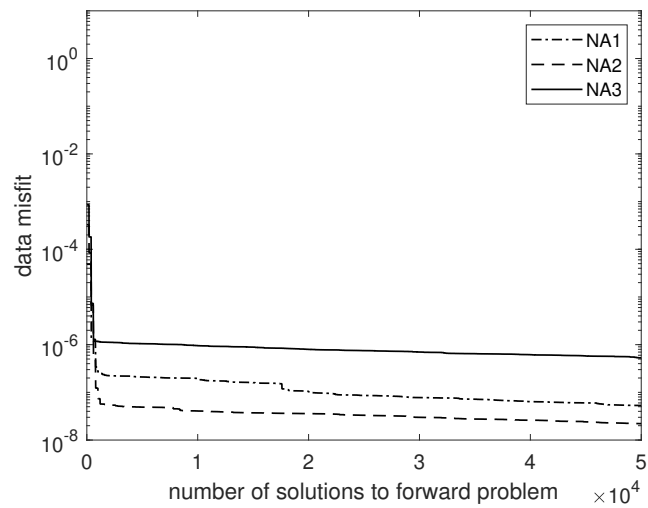
We compare the three algorithm in Figure 5, where the misfit function is plotted against the number of models for which the forward problem has been solved. There are three runs in each case. We note that the misfit reduction of NA has a more favorable character, exhibiting more large steps in the early stage. As a result, two of the three NA curves have lower data misfits than the best SA and GA curves. Therefore, with the specific details we design for the three algorithms, NA is most efficient and is therefore selected for our further study on larger models.



(a)



(b)



(c)

FIG. 5. Data misfit reduction for three runs of (a) SA, (b) GA, and (c) NA.

Noise test on pseudo-well logs

In this section we test the robustness of the method in the presence of additive random noise. We generate pseudo-well-logs of P , C and S_w , and use them to compute the logs of V_P , V_S and ρ based on the KT model. These logs are denoted by the black solid lines in Figure 6. If the exact velocity and density logs are used as input data for the rock physics inversion, the P and C logs can be accurately reconstructed, whereas the S_w estimate exhibit visible oscillation around the true model. As mentioned in the previous section, this is due to the very low sensitivity of velocities and density to S_w . Nonetheless, the S_w estimate is acceptable since it captures the major structures.

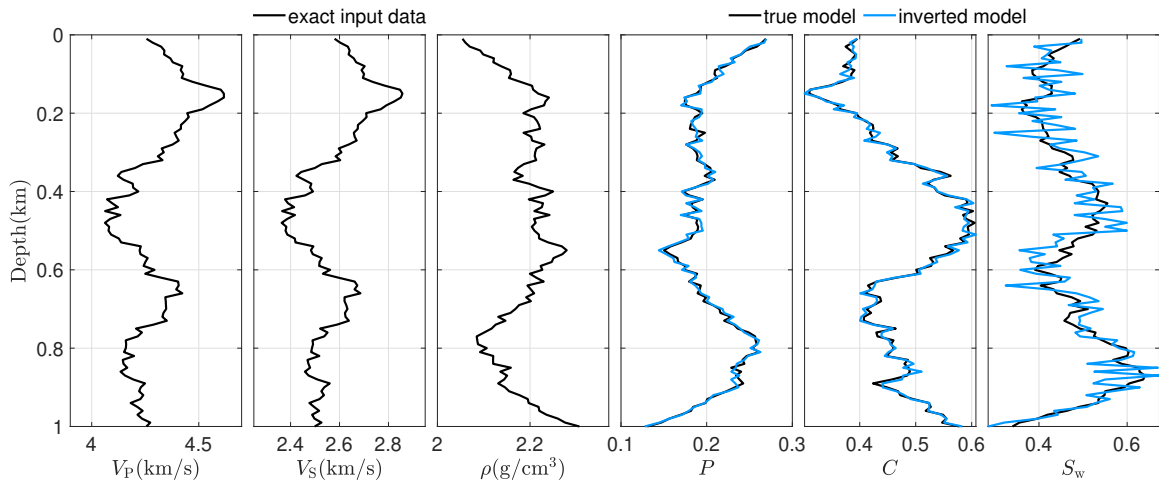


FIG. 6. Test with noise-free data. The back lines denote the true models and the blue lines denote the inverted models. The true elastic models are used as input data for the rock physics inversion.

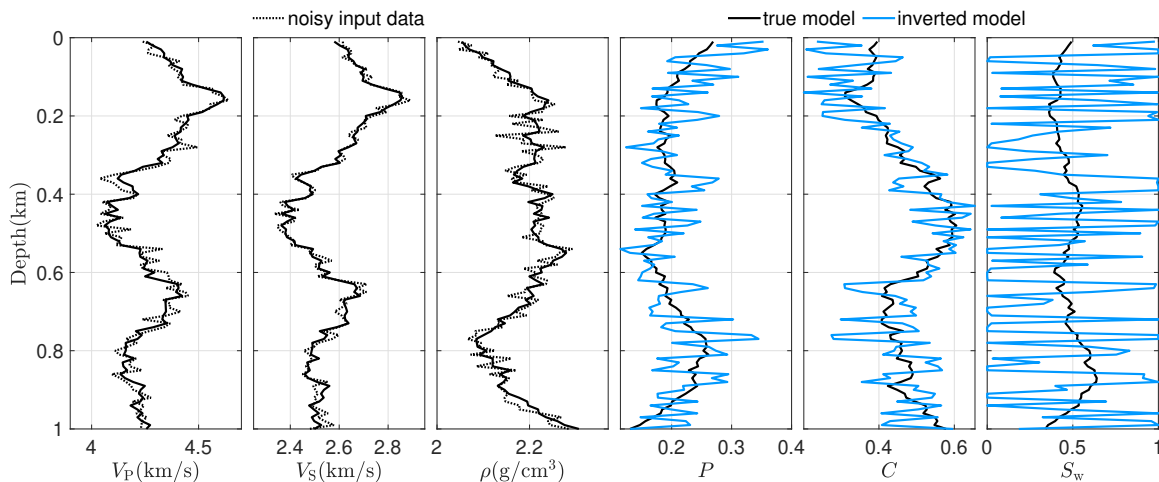


FIG. 7. Test with noisy data. Mild Gaussian noises are added to the elastic models, as denoted by the black dashed lines. The blue lines denote the inverted models.

However, after we add some mild Gaussian noise to the input data, as denoted by the black dashed line in Figure 7, the inverted rock physics properties become far from satisfactory. The relatively small errors as they appear in the elastic model are magnified

significantly in the P , C and Sw recoveries. The estimate of Sw appears to fair the worst, covering the entire search space. We conclude that the simultaneous inversion of the three rock physics parameters is ill-conditioned (i.e., lack of stability and robustness), as the model is very sensitive to the errors in the data.

Given that it is difficult to invert the whole set of (P, C, Sw) from noisy data, we introduce prior information to the inversion, expecting to make it better-posed. We assume the exact Sw is known, which is clearly a favorable case, and we invert only P and C . The result is shown in Figure 8. We observe a significant improvement in the P and C recoveries, which exhibit mild oscillation around the true model.

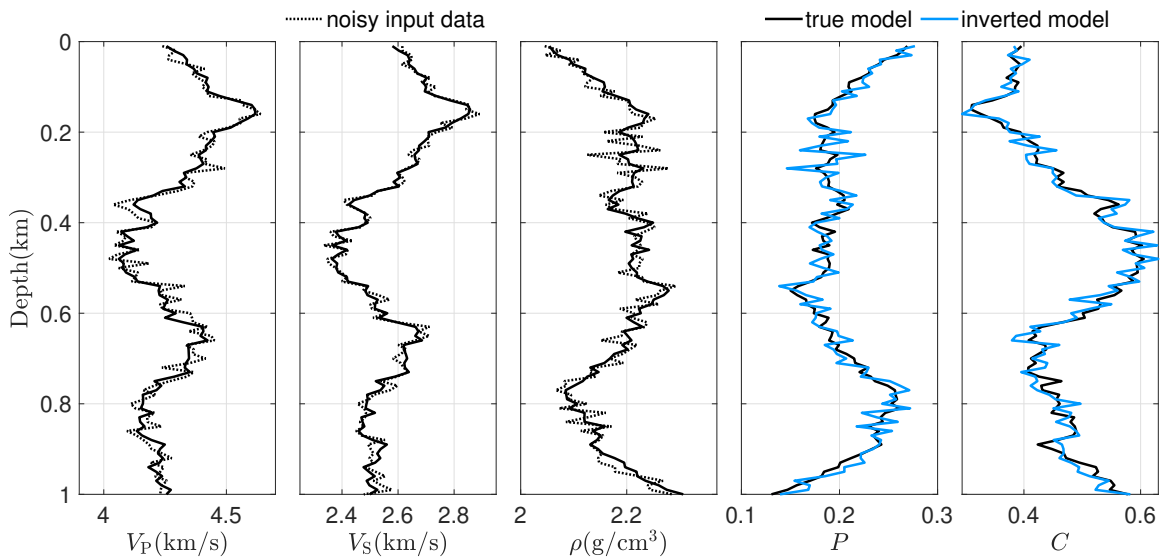


FIG. 8. Test with noisy data. Only porosity and clay content are inverted, assuming a priori information of the exact water saturation model

Rock physics inversion using EFWI results

In this section we present synthetic example to combine the high-resolution result of EFWI with the rock physics inversion using the proposed global optimization method. For the EFWI algorithm, a 2D, frequency-domain, three parameter elastic inversion is set up. We select a $1\text{km} \times 1\text{km}$ part of the elastic Marmousi2 model and assign rock physics property values to each cell. Figure 9 shows the true elastic model, the initial model which is a smoothed version of the true model, and the EFWI result. We observe that although the deeper part of the elastic model is slightly underestimated, the inversion result is reasonably accurate, capturing the main structures. The recovered elastic model is next used as input data for the rock physics inversion.

In Figure 10 we plot the true porosity and clay content models, which are connected to the true elastic model via the KT relation, and the inverted P and C models. Again, the inversion is achieved via a point-by-point conversion from the elastic model to the rock physics properties using the neighborhood algorithm. We observe that both the structure and values of the P model are well recovered. The inverted C model, on the other hand, recovers the structure reasonably well but exhibits visible areas either overestimated or

underestimated. This likely originates from the errors in the EFWI-derived elastic model, as shown in the vertical profiles in Figure 11.

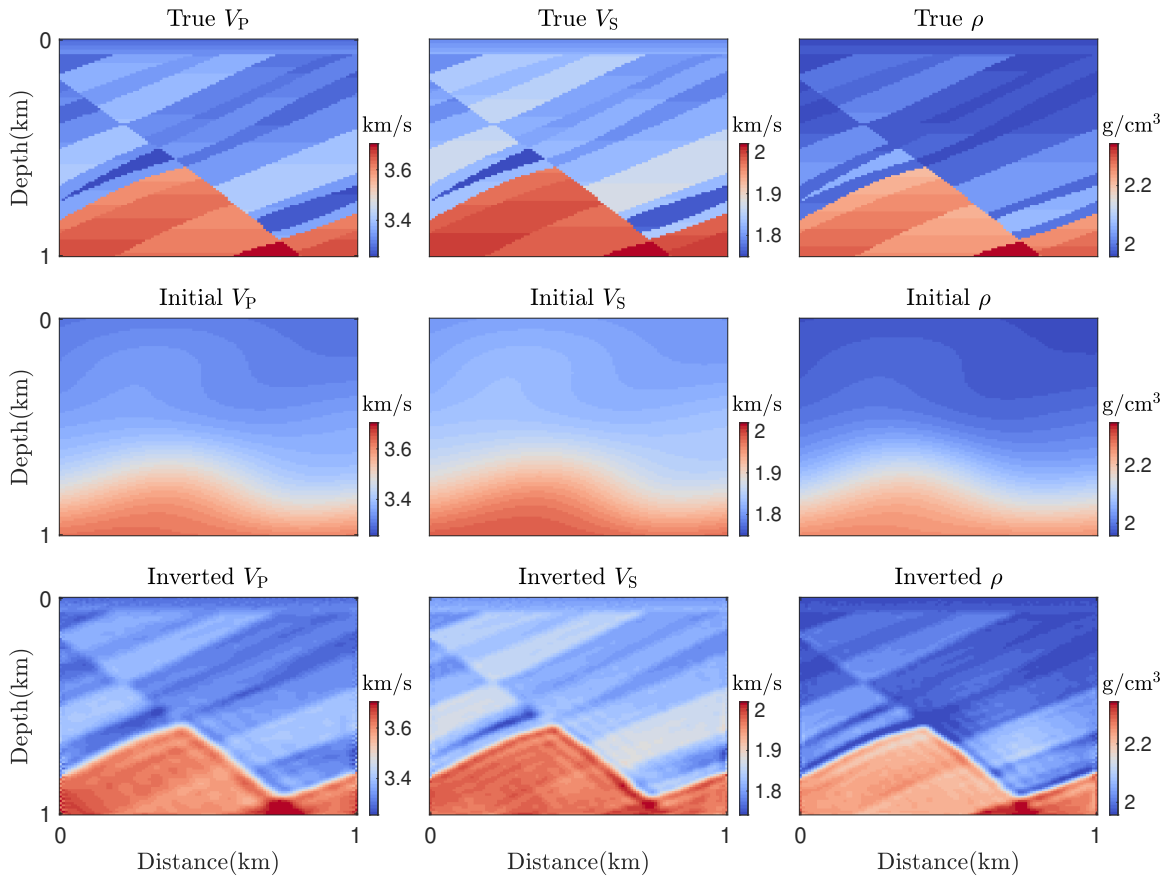


FIG. 9. True and initial elastic models and the corresponding EFWI results.

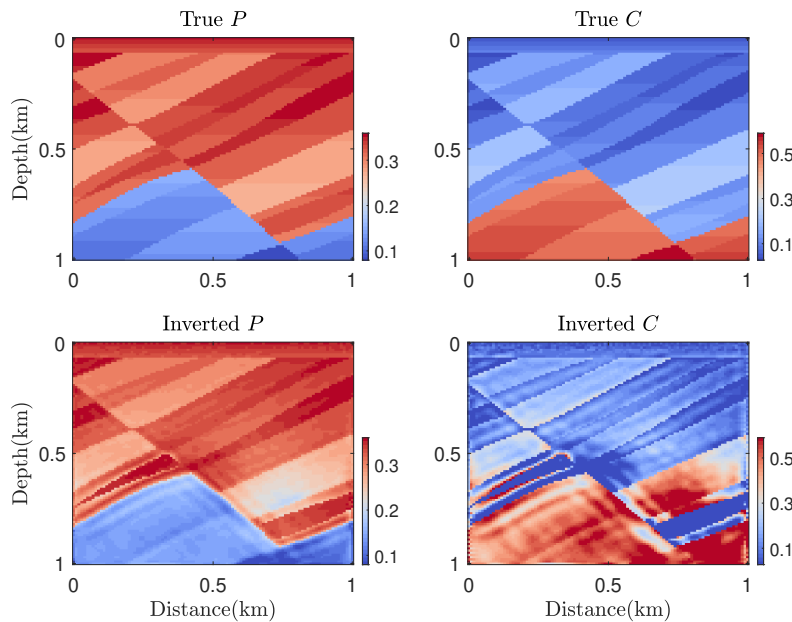


FIG. 10. True models of porosity and clay content and the corresponding inverted models.

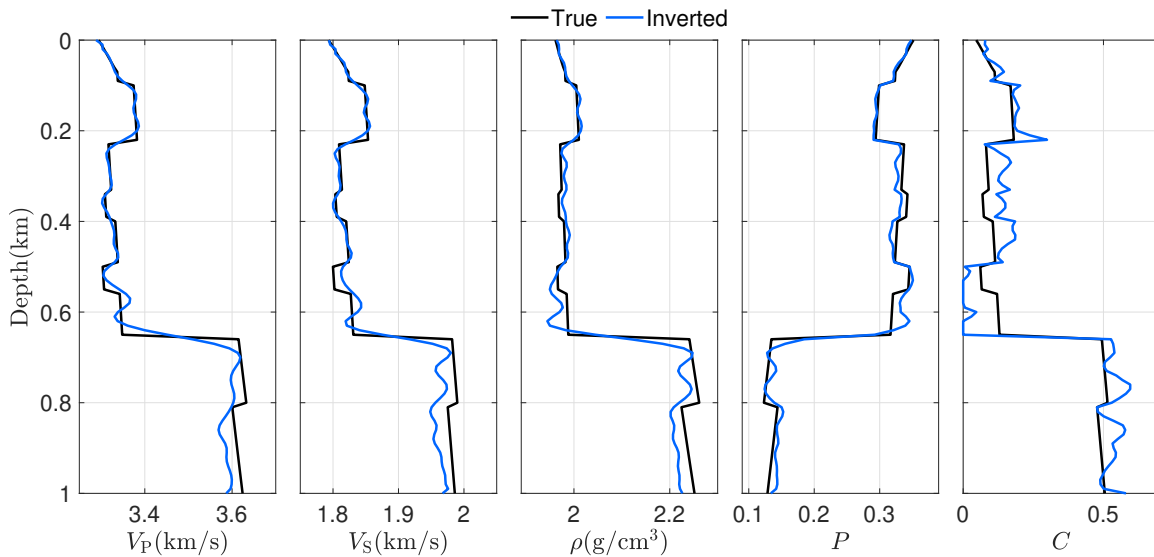


FIG. 11. Vertical profiles of the true and inverted models at lateral position 0.5km. The inverted elastic models from EFWI are used as input data for the inversion of rock physics properties.

CONCLUSIONS

In this work we studied three global optimization methods: simulated annealing, genetic algorithm, and neighborhood algorithm for a rock physics inversion problem: inverting porosity, clay content, and water saturation from velocities and density. We found that the neighborhood algorithm is more efficient in reducing data misfit for the experiment we set up, however this conclusion may vary with user-defined parameters of the algorithms. We illustrated that the simultaneous inversion of the three rock physics parameters is ill-conditioned because it is very sensitive to the errors in the data. We then created a favorable scenario by using the exact water saturation as a priori information and only invert for porosity and clay content. This makes the inversion of the two parameters stable with noisy data. The proposed approach can be combined with EFWI for a sequential inversion for rock physics properties: first the elastic attributes are estimated using EFWI, they are next transformed to rock physics properties using the global optimization method.

ACKNOWLEDGMENTS

We thank the sponsors of CREWES for continued support. This work was funded by CREWES industrial sponsors, and NSERC (Natural Science and Engineering Research Council of Canada) through the grant CRDPJ 461179-13 and CRDPJ 543578-19. Qi Hu was also supported by the SEG/James L. Allen Scholarship.

REFERENCES

- Bosch, M., Mukerji, T., and Gonzalez, E. F., 2010, Seismic inversion for reservoir properties combining statistical rock physics and geostatistics: A review: *Geophysics*, **75**, No. 5, 75A165–75A176.
- Brossier, R., Operto, S., and Virieux, J., 2009, Seismic imaging of complex onshore structures by 2D elastic frequency-domain full-waveform inversion: *Geophysics*, **74**, No. 6, WCC105–WCC118.
- Buland, A., and Omre, H., 2003, Bayesian linearized AVO inversion: *Geophysics*, **68**, No. 1, 185–198.

- Doyen, P., 2007, Seismic reservoir characterization: An earth modelling perspective, vol. 2: EAGE publications Houten.
- Dupuy, B., Garambois, S., and Virieux, J., 2016, Estimation of rock physics properties from seismic attributes—part 1: Strategy and sensitivity analysis: *Geophysics*, **81**, No. 3, M35–M53.
- Grana, D., 2016, Bayesian linearized rock-physics inversion: *Geophysics*, **81**, No. 6, D625–D641.
- Kuster, G. T., and Toksöz, M. N., 1974, Velocity and attenuation of seismic waves in two-phase media: *Geophysics*, **39**, No. 5, 587–618.
- Mavko, G., Mukerji, T., and Dvorkin, J., 2009, *The rock physics handbook: Tools for seismic analysis of porous media*: Cambridge university press.
- Nocedal, J., and Wright, S., 2006, *Numerical optimization*: Springer Science & Business Media.
- Pan, W. Y., Innanen, K. A., and Geng, Y., 2018, Elastic full-waveform inversion and parametrization analysis applied to walk-away vertical seismic profile data for unconventional (heavy oil) reservoir characterization: *Geophysical Journal International*, **213**, No. 3, 1934–1968.
- Sambridge, M., 1999, Geophysical inversion with a neighbourhood algorithm—I. searching a parameter space: *Geophysical journal international*, **138**, No. 2, 479–494.
- Sen, M. K., and Stoffa, P. L., 2013, *Global optimization methods in geophysical inversion*: Cambridge University Press.
- Tarantola, A., 2005, *Inverse problem theory and methods for model parameter estimation*: SIAM.